12-8-2000

Atmospheric CO2 evasion, dissolved inorganic carbon production, and net heterotrophy in the York River estuary

Peter Raymond

James E. Bauer
Virginia Institute of Marine Science

Jonathan Cole

Recommended Citation

Raymond, Peter; Bauer, James E.; and Cole, Jonathan, Atmospheric CO2 evasion, dissolved inorganic carbon production, and net heterotrophy in the York River estuary (2000). *Limnology and Oceanography*, 45(8), 1707-1717.
https://doi.org/10.4319/lo.2000.45.8.1707

Limnol. Oceanogr., 45(8), 2000, 1707–1717

Atmospheric CO_2 evasion, dissolved inorganic carbon production, and net heterotrophy in the York River estuary

Peter A. Raymond[1] *and James E. Bauer*
School of Marine Science, College of William and Mary, Gloucester Point, Virginia 23062

Jonathan J. Cole
Institute of Ecosystems Studies, Millbrook, New York 12545

Abstract

Direct measurements of the partial pressure of CO_2 (pCO_2) and dissolved inorganic carbon (DIC) were made over a 2-yr period in surface waters of the York River estuary in Virginia. The pCO_2 in surface waters exceeded that in the overlying atmosphere, indicating that the estuary was a net source of CO_2 to the atmosphere at most times and locations. Salinity-based DIC mixing curves indicate there was also an internal source of both DIC and alkalinity, implying net alkalinity generation within the estuary. The DIC and alkalinity source displayed seasonal patterns similar to that of pCO_2 and were reproducible over a 2-yr study period.

We propose that the source of inorganic carbon necessary for both the sustained CO_2 evasion to the atmosphere and the advective export of DIC is respiration in excess of primary production (e.g., net heterotrophy). The rates of CO_2 evasion and DIC export were estimated to provide an annual rate of net heterotrophy of $\sim$100 g C m^{-2} yr^{-1}. Approximately 40% of this excess inorganic carbon production was exported as DIC to the coastal ocean, whereas 60% was lost as CO_2 evasion to the atmosphere. The alkalinity generation needed to sustain the export of inorganic carbon, as HCO_3^-, is most likely provided by net sulfate reduction in sediments. Accumulation of sulfide in the sediments of a representative site directly adjacent to the York River estuary is sufficient to account for the net export of alkalinity. The seasonality of net heterotrophy causes large variations in annual CO_2 and DIC concentrations, and it stresses the need for comprehensive temporal data sets when reporting annual rates of CO_2 evasion, DIC advection, and net heterotrophy.

The metabolic state of an ecosystem represents the balance between gross primary production (GPP) and total respiration (R; Kemp et al. 1997). In heterotrophic systems, R $>$ GPP as a result of the breakdown of allochthonous organic material and the remineralization of inorganic nutrients and carbon (as CO_2). In autotrophic systems, GPP $>$ R, resulting in the export or burial of organic matter through the conversion of inorganic nutrients and carbon dioxide by photosynthesis. In an estuary, the linkage between net metabolism and carbon and nutrient cycling will alter the quantity, quality, and species of carbon, nitrogen, and phosphorus reaching the coastal oceans.

Photosynthesis is dependent, in part, on the availability of inorganic nutrients, whereas respiration is dependent on the availability of labile organic material. Thus, the metabolic state of an estuary is also inherently linked to the delivery of allochthonous inorganic nutrients and labile organic material (Hopkinson and Vallino 1995; Smith and Hollibaugh 1997). The delivery of nutrients and organic material to estuaries is rarely in steady state; it may change dramatically over short time scales because of events such as rain events and storms (Magnien et al. 1992). Furthermore, processes such as flocculation (Sholkovitz et al. 1978), desorption (Mayer et al. 1998), sedimentation, pycnocline development, light limitation on phytoplankton (Cloern 1987), and the mixing of freshwater and seawater create complex carbon and nutrient dynamics within estuaries. As a result of this complexity, estimates of metabolism in estuaries are difficult to assess, and few comprehensive studies of it have been undertaken (Smith and Hollibaugh 1993; Heip et al. 1995; Gattuso et al. 1998).

A summary of the methods presently used for estimating metabolism in coastal and estuarine systems can be found in Smith and Hollibaugh (1993). One method involves the measurement of inorganic carbon species, because the cycling of inorganic carbon is related to the metabolic state of an estuary through the production and utilization of CO_2 during photosynthesis and respiration. In fact, Smith and Hollibaugh (1993) state that the most satisfactory approach to estimating net metabolism in the coastal ocean might be the detailed analysis of CO_2 in surface waters.

Recently, CO_2 supersaturation in estuaries has been reported for a number of different systems (Raymond et al. 1997; Cai and Wang 1998; Frankignoulle et al. 1998), indicating net heterotrophy; yet, a detailed description and analysis of the spatial and temporal variability of CO_2 and dissolved inorganic carbon (DIC) distributions and fluxes in

[1] To whom correspondence should be addressed. Present address: The Ecosystems Center, Marine Biological Lab, Woods Hole, Massachusetts 02543 (praymond@mbl.edu).

Acknowledgments

We would like to thank H. Ducklow, I. Anderson, K. Moore, S. V. Smith, and an anonymous reviewer for comments on this manuscript. We are grateful to M. Church, L. McCallister, M. Schrope, and A. Loh for help in the field.

This work was supported by the Ocean Margins Program of the U.S. Department of Energy (grant DE-FG05-94ER61833) and the Chemical Oceanography Program of the U.S. National Science Foundation (grant OCE-9501531).

estuaries is lacking. More importantly, CO_2 supersaturation is only qualitative evidence for net heterotrophy. Estuarine CO_2 may have sources and fates other than net heterotrophy and atmospheric exchange, and for a quantitative and convincing estimate of system metabolism, a robust data set of concurrent surface water CO_2 and DIC measurements is necessary. Another notable source of estuarine CO_2 is supersaturated riverine waters, and therefore, quantitative information that estuarine CO_2 supersaturation is balanced by internal net heterotrophy is necessary.

Apart from atmospheric evasion, the inorganic carbon produced by net heterotrophy can also be exported advectively as DIC in the form of bicarbonate (HCO_3^-). Raymond et al. (1997) used a comprehensive temporal and spatial data set to quantify CO_2 evasion and DIC export in the tidal freshwater Hudson River, and they concluded that DIC export was not a significant sink for CO_2 generated from net heterotrophy. In order to convert CO_2 produced by net heterotrophy to bicarbonate, a source of alkalinity must be present. Estuarine systems receive large quantities of sulfate from seawater mixing, and sulfate reduction can balance CO_2 conversion to bicarbonate (Smith and Hollibaugh 1997). We propose that sulfate reduction may be an important sink for CO_2 produced by net heterotrophy in the York River estuary.

This paper represents a novel approach for elucidating and quantitatively estimating patterns of net metabolism in the York River estuary by using spatial and seasonal dynamics of atmospheric CO_2 exchange and DIC dynamics. We show that in the York, the advective export of excess DIC from net heterotrophy is of equal importance to CO_2 gas evasion when using inorganic carbon dynamics to estimate net heterotrophy for the entire system.

Materials and methods

Description of study area—The York River estuary is a subestuary of the Chesapeake Bay and is formed by the convergence of the Pamunkey and Mattaponi Rivers 50 km from its mouth (Fig. 1). The Pamunkey contributes approximately 70% of the total flow to the York, and it is flanked by tidal freshwater marshes, with some individual marshes being greater than 4 km^2 in size. The York River estuary is considered pristine amongst the subestuaries of the Chesapeake Bay, with the only industry being a paper plant at the convergence of the Pamunkey and Mattaponi.

Previous work has focused primarily on the mouth of the estuary, concentrating on the effects of stratification–destratification caused by spring-neap cycles (Haas et al. 1981; Ducklow 1982). More recently, bacterial dynamics (Koepfler 1989; Schultz 1999) and phytoplankton and nutrient dynamics (Sin et al. 1999) have been studied in the main part of the York River estuary. Bacterial production has been found to increase with decreasing salinity (Koepfler 1989; Schultz 1999), and it is directly related to temperature, with production rates being three-fold greater in warm than in cold months (Koepfler 1989). Phytoplankton exhibit distinct winter/spring blooms in the mesohaline portions of the York system and smaller summer blooms in the upper York (Sin et al. 1999).

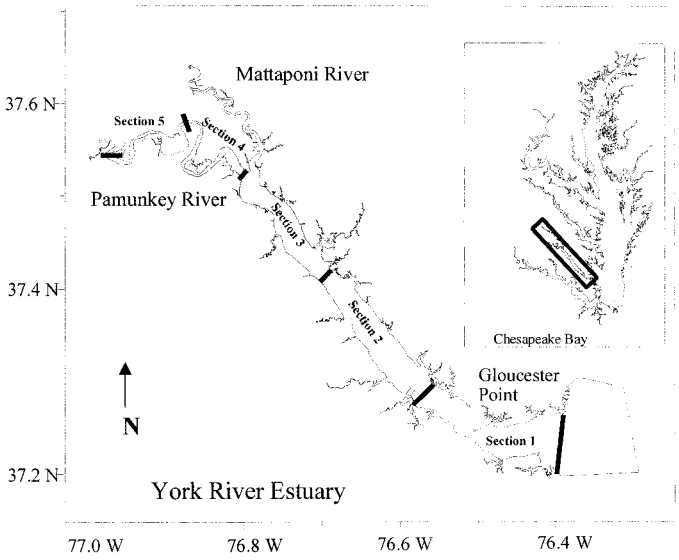

Fig. 1. Map of York River estuary and surrounding region. The York River estuary was broken into five 10-nautical-mile sections to estimate CO_2 flux. The first three sections are located in the lower York estuary, whereas sections 4 and 5 are located on the Pamunkey River, which discharges most of the freshwater into the lower York.

Twelve sampling transects for DIC and the partial pressure of CO_2 (pCO_2) were performed between the mouth of the York and the point at which freshwater was encountered. The salinity at the mouth ranged from 14 to 23.5. Sampling sites were not fixed in location, but instead were sampled to provide adequate coverage of salinity.

pCO_2 measurements—In order to model the flux of CO_2 and examine CO_2 dynamics in the York River estuary, the pCO_2 in surface waters (~0.5-m depth) was measured a total of 99 times on 12 transects from July 1996 to December 1997. The pCO_2 is equal to $[CO_2]/\alpha$, where α is the CO_2 solubility coefficient, and it was measured according to the method of Cole et al. (1994). Two 0.5-liter gas-tight bottles were filled with unfiltered sample water, 25 ml of air was introduced, and the bottle was shaken 100 times to force the air into equilibrium with the water sample. Each air headspace was subsampled into two 20-ml syringes and returned to the laboratory for gas analysis. CO_2 gas was analyzed on a Li-Cor LI6252 or a Beckman model 880 infrared gas analyzer by using a flow-through system with ultra-high purity helium gas as the carrier. Samples were analyzed on the same day they were collected, along with multiple sets of 0, 400, 1000, and 10,000 ppmv CO_2 gas standards. The average coefficient of variation for this procedure was 7% of the mean for duplicates.

Dissolved inorganic carbon measurements—On 12 transects between July 1996 and April 1998, 100 surface water measurements of DIC were made along the salinity gradient of the York River estuary. Duplicate water samples were collected in 7-ml gas-tight test tubes and stored on ice and in the dark while in the field and were analyzed in the laboratory within 12 h of sampling. DIC concentrations were

measured on a Shimadzu TOC 5000A in inorganic carbon mode, and they were calibrated with 0, 500, 800, 1,000, and 2,200 μM $NaHCO_3$ standards. The average coefficient of variation for this procedure was 4% of the mean for duplicates.

Atmospheric exchange calculation—The gas exchange coefficient (k) and the concentration gradient govern the flux (in mmol m^{-2} s^{-1}) of CO_2 across the air–water interface as follows:

$$\text{Flux} = k([CO_2]_{\text{water}} - [CO_2]_{\text{air}}) \quad (1)$$

where k (m s^{-1}) is the gas exchange coefficient for CO_2 at a given temperature and salinity. The term $[CO_2]_{\text{water}} - [CO_2]_{\text{air}}$ is the concentration gradient (mmol m^{-3}) between the water and the air. In order to estimate k, we modeled k as a function of wind speed using data from two estuarine studies that measured directly k and the wind speed in tidal systems (Clark et al. 1994, Carini et al. 1996). Both studies modeled k as a function of wind speed and reported values of k for a gas with a Schmidt number of 600 (k_{600}), which is the Schmidt number for CO_2 at 20°C. We fit the individual data points from these studies with the following power function:

$$k_{600} = 2.78U_{10}^{0.46}, \quad (2)$$

where U_{10} is the wind speed recorded at 10 m ($r^2 = 0.43$; $P < 0.03$; $n = 11$). Once k_{600} has been established, k for CO_2 (k_{CO_2}) can be calculated by the ratio of the Schmidt numbers using the following equation (Jahne et al. 1987):

$$k_{600}/k_{CO_2} = (600/Sc_{CO_2})^n. \quad (3)$$

The Schmidt numbers for CO_2 (Sc_{CO_2}) for given temperatures and salinities were calculated with the relationships in Wanninkof (1992). The exponent n can vary from unity to -0.67, depending on the process that dominates diffusion; an estimate of -0.5 (Jahne et al. 1987) was used for this study.

In order to determine spatial variations in CO_2 flux, the estuary was subdivided into five sections of 10 nautical miles each (Fig. 1). The concentration gradient in Eq. 1 was estimated by using direct measurements of pCO_2 and an atmospheric pCO_2 concentration of 380 ppmv. For each transect, a minimum of one site was located within each section of 10 nautical miles. When multiple sites were located in a section, concentrations were averaged. Based on the predictable seasonal changes in pCO_2 observed in this study, changes in CO_2 concentrations for a given section between two sampling dates were assumed to be linear, allowing for the calculation of daily fluxes for each section for the entire sampling period.

In order to report CO_2 fluxes as an integrated whole estuary flux, the fluxes for each section of the York were normalized to sectional areas using the surface areas reported by Cronin (1971). For the Pamunkey River (upper York), the surface area of tidal marshes could not be ignored because each meander of the Pamunkey (Fig. 1) is occupied by large stretches of tidal marsh that are inundated with river water twice a day. We therefore tabulated the surface areas for the marshes using reports by Doumelele (1979), and Silberhorn and Zacherle (1987), and divided by 2 (because they are only inundated during high tides) and included this area in the surface areas of sections 4 and 5. The fluxes from each section were then summed to obtain an integrated daily flux for atmospheric exchange in the York River estuary system.

Estimating fluxes of DIC—Mixing curves of DIC versus salinity were used to estimate how much DIC is added by net heterotrophy during estuarine transport. Mixing curves are a commonly used approach for interpreting net source/sink dynamics of estuarine constituents (for examples, *see* Officer 1979; Loder and Reichard 1981; Kaul and Froelich 1984). When observed values fall on the linear mixing curve, it is generally interpreted that the constituent of interest mixes conservatively with respect to the system's residence time. In contrast, values falling above the conservative mixing curve are indicative of a net internal source, whereas values falling below indicate a net internal sink for the constituent being examined.

Kaul and Froelich (1984) presented a model that uses mixing curves to estimate the internal flux of a dissolved constituent. When the distribution of a dissolved constituent is continuous and predictable with simple polynomial equations, the flux (mmol s^{-1}) of that dissolved constituent within the estuary is defined as

$$\text{Input flux} = Q(C_s - C_O), \quad (4)$$

where Q is freshwater flow (m^3 s^{-1}), C_O (μM) is where the polynomial equation defining DIC concentrations intersects the y-intercept (or the concentration at zero salinity), and C_s (μM) is the concentration of the constituent where the tangent at the seawater end-member crosses the y-intercept. For our purposes, when an estuarine source of DIC was present, we modeled each mixing curve with a second-order polynomial. We used the polynomial equation to define the tangent and calculate the y-intercept for the tangent at the seawater end-member. According to Kaul and Froelich (1984), the total export flux from the estuary is the product of C_s and flow, the internal flux is the product of $C_s - C_O$ and flow, and the flux from the freshwater end-member is the product of C_O and flow. In order to express these fluxes in terms of a rate in mmol m^{-2} d^{-1}, we converted seconds to days, and the flux was divided by the surface area used to define our system's boundaries (i.e., the same surface area used in the atmospheric evasion estimate outlined above).

Supplemental data—In addition to our measured values for the York, pCO_2 was calculated for the James, Rappahannock, and Potomac estuaries for the 1997 water year from data available on the Environmental Protection Agencies (EPA) Chesapeake Bay program Web site (http://www.chesapeakebay.net/bayprogram). Alkalinity, pH, temperature, and salinity were used to calculate pCO_2 according to equations found in Millero (1995). The following EPA stations were used for each estuary: LE 5.4, LE 5.3, LE 5.2, LE 5.1, RET 5.2, TF 5.6, and TF 5.5A for the James; LE 3.2, LE 3.1, RET 3.1, RET 3.2, TF 3.3, TF 3.2, and TF 3.2 for the Rappahannock; and RET 2.4, RET 2.3, RET 2.2, and RET 2.1 for the Potomac.

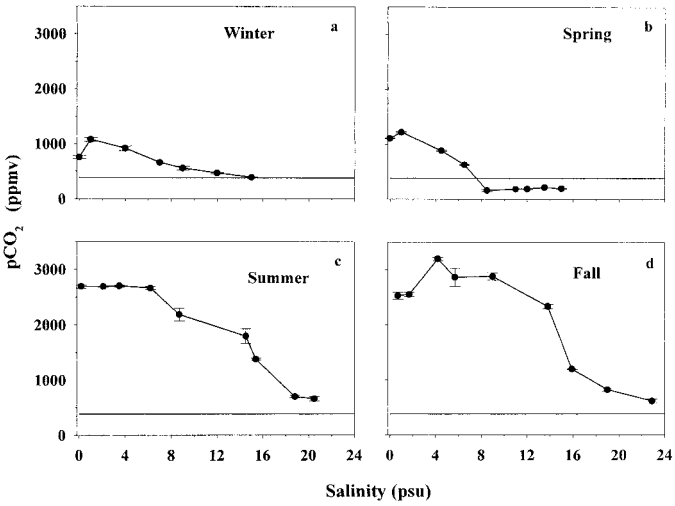

Fig. 2. (a)–(d) Seasonal examples of surface water pCO_2 in the York River estuary plotted as a function of salinity. The pCO_2 was generally higher at low salinities and reached a late summer and early fall maximum. Winter: 17 Jan 97; Spring: 19 Mar 97; Summer: 18 Jul 97; Fall: 25 Sep 97. Each point is an average of two duplicate samples. The horizontal line represents atmospheric pCO_2 values of ~380 ppmv.

Results

pCO_2: spatial and temporal patterns and atmospheric exchange—The York River estuary was dominated by supersaturated pCO_2 conditions. The average (with SD) pCO_2 measured at a total of 99 surface sites was 1,070 ± 867 ppmv, with a maximum of 3,467 ppmv in July 1996 in section 4 of the estuary, and a minimum of 113 ppmv in April of 1997 in section 2. Of the 99 total measurements, 21 were undersaturated with respect to the atmosphere, and all except one of these undersaturated samples were taken from sections 1 or 2. For the estuary sections depicted in Fig. 1, the average salinity for sections 1–5 was 17.5, 13.4, 10.5, 4.8, and 1.1, respectively, whereas the average pCO_2 was 468, 416, 763, 1,886, and 1,818 ppmv, respectively.

The pCO_2 values in the York River estuary displayed pronounced spatial and temporal variations. Spatially, pCO_2 decreased with increasing salinity, with the gradient being stronger in the summer and fall months (Fig. 2). Low salinity sections 4 and 5 had high average pCO_2 values; section 3 was a transitional zone showing intermediate pCO_2 levels, whereas the lower estuary (sections 1 and 2) had the lowest pCO_2 values. Temporally, pCO_2 levels were lowest in winter and early spring (Fig. 2a,b) and highest in the late summer and early fall (Figs. 2c,d). The most pronounced seasonal variation occurred in the lower salinity portions of the York (Fig. 2a–d).

Calculated evasion rates for CO_2 along the York River estuary are shown in Table 1. Temporal and seasonal variation in gas exchange generally correlated with pCO_2 distributions, with exchange generally being greatest at low salinities and during summer and fall months (Table 1). The whole-estuary flux was much lower than fluxes in the upper river (sections 4 and 5), because the lower sections have larger surface areas and lower pCO_2 concentrations. Negative fluxes (pCO_2 invasion) were calculated for winter months in section 1 (Table 1). The weighted annual average rate of CO_2 evasion for the period of July 1996 to July 1997 was 52.7 g C m^{-2} yr^{-1}, and it rose to 75.1 g C m^{-2} yr^{-1} if the period between December 1996 and December 1997 was considered. The July 1996 to July 1997 and December 1996 to December 1997 rates for the upper York (section 5) were 202.8 and 235.3 g C m^{-2} yr^{-1}, respectively, and for the lower York (section 1) they were 5.0 and 9.7 g C m^{-2} yr^{-1}, respectively.

DIC: spatial and temporal trends—Surface DIC measurements were made along the salinity gradient of the York River estuary from July 1996 to April 1998. When mixing curves were generated for individual transects, a strong seasonal pattern in the nonconservative behavior of DIC developed (Fig. 3a–l). In July 1996 (Fig. 3a), a large DIC anomaly occurred in the middle reaches of the estuary, where measured DIC concentrations fell above the mixing curve. In Fall 1996, the anomaly was still present, but DIC concentrations approached the conservative mixing line. In Spring 1997, DIC mixed conservatively. The patterns ob-

Table 1. CO_2 flux estimates (mmol m^{-2} d^{-1}) for the York River estuary. The k values used for these estimates were obtained using Equation 2 (see text) and daily wind speeds. Positive fluxes are from the estuary to the atmosphere (evasion). Whole estuary fluxes were obtained by multiplying each section's flux by its surface area, summing the five section fluxes, and dividing by the surface area of the entire estuary. Surface areas are (all 10^6 m^2) 58.4, 58.6, 39.0, 12.6, and 11.3 for sections 1–5, respectively.

Period	Section 1 flux	Section 2 flux	Section 3 flux	Section 4 flux	Section 5 flux	Whole estuary flux
10 Jul 96–07 Sep 96	8.0	12.9	10.0	98.0	68.1	23.1
08 Sep 96–18 Nov 96	3.6	0.7	8.5	73.5	69.0	11.0
19 Nov 96–22 Jan 97	−2.1	0.5	7.8	47.8	35.1	6.1
23 Jan 97–24 Mar 97	−5.6	4.9	6.1	32.5	18.1	6.9
25 Mar 97–13 Apr 97	−3.3	7.2	6.2	38.3	18.0	9.5
14 Apr 97–22 Jun 97	1.6	6.4	9.1	36.9	35.8	10.5
23 Jun 97–16 Jul 97	4.1	18.6	12.8	80.9	93.0	27.6
17 Jul 97–22 Sep 97	8.3	27.3	14.7	81.9	107.3	36.1
23 Sep 97–29 Oct 97	7.7	19.7	15.1	73.2	72.5	27.0
30 Oct 97–12 Dec 97	4.8	7.0	15.1	37.0	45.1	12.2

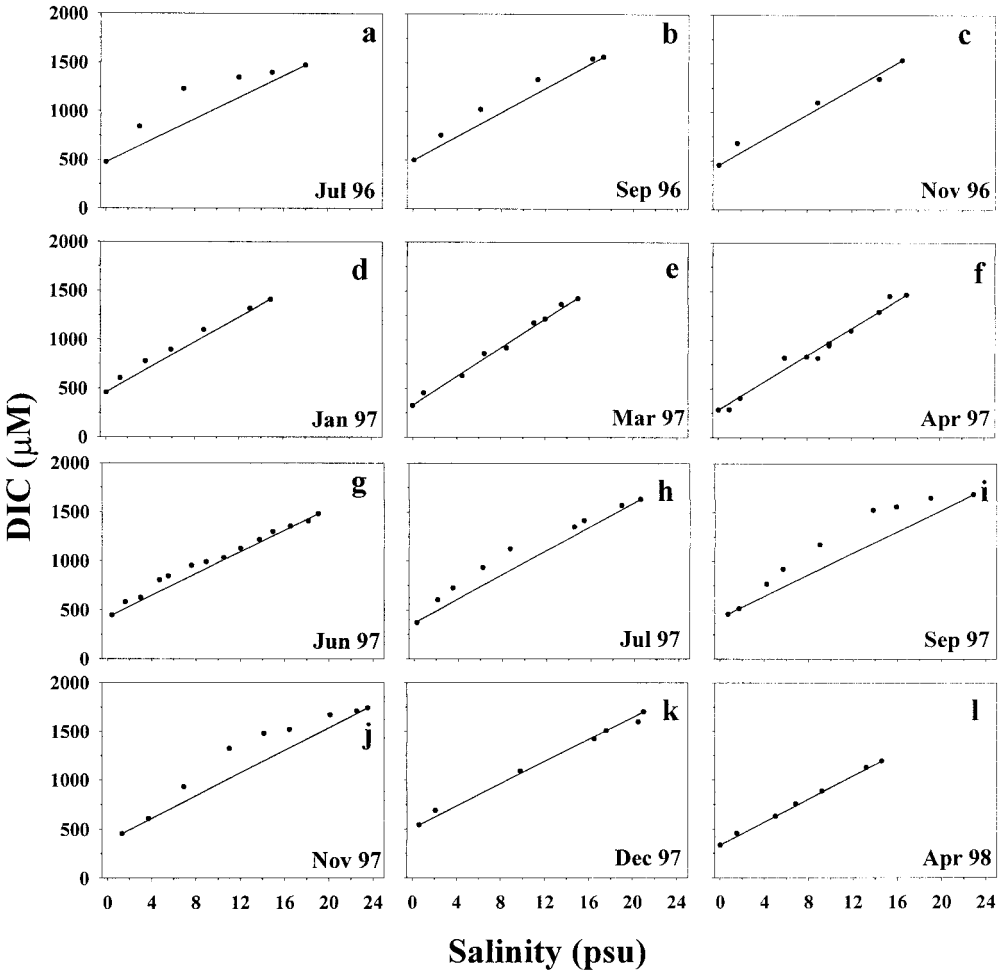

Fig. 3. (a)–(l) Dissolved inorganic carbon distributions in the York River estuary. The mixing curves indicate that an estuarine source of DIC followed pronounced seasonal variation and repeated itself over the 2-yr study period. Each point represents the average of two samples, and the average coefficient of variation for the duplicate samples was 4% of the mean.

served in 1996–1997 were repeated during the 1997–1998 sampling period with positive anomalies in DIC mixing curves in the summer and fall, followed by conservative mixing in the winter and spring.

The DIC mixing curves (Fig. 3a–l) were readily reproduced with polynomial equations (Table 2). This allowed for the calculation (with Eq. 4) of the advective export of the DIC that was added during estuarine transport and the examination of the relative magnitude and temporal variation in this inorganic carbon sink. There are, however, several shortcomings involved with interpreting mixing curves. The main problem is that the constituent being examined is assumed to be in steady state with respect to freshwater residence time. Because mixing curves are generated from concentrations at the freshwater and mouth stations, sudden large variations (i.e., non–steady state behavior) in end-member concentrations can affect the slope of a mixing curve (Loder and Reichard 1981), making a parameter appear nonconservative when in fact it is conservative. In the York River estuary, DIC at the freshwater end-member (C_O, in Table 2) varied seasonally; freshwater DIC concentrations decreased during high flow periods in the winter and spring months. The winter/spring decline in freshwater DIC concentrations does not affect our calculation because mixing curves indicate that there is a DIC source during the summer and fall months only (Fig. 3a–l). The average (with SD) freshwater concentration for summer and fall months was 407.8 ± 69.4, whereas the average change between sampling periods was 46.8 ± 37.9. These changes are small compared with the large differences between C_s and C_O in Table 2, and therefore, they have little effect on the calculation of added DIC.

The concentrations of DIC added to the York during estuarine transport ($C_s - C_O$; Eq. 4) were high in summer and fall, and low (sometimes zero) in winter and spring, whereas flow rates in the York were low in summer and fall and high in winter and spring. High flow rates combined with negligible amounts of DIC added during the winter and spring make this period important when considering the total flux of DIC out of temperate estuaries. The DIC added during estuarine transport ranged from 0% to 76% of the total flux and averaged (with SD) 42% ± 30%. We calculated annual

Table 2. DIC distributions and fluxes in the York River estuary. Equations are polynomial equations used to fit the data from DIC versus salinity transects displayed in Fig 3. All equations have $r^2 > 0.98$ and $P < 0.01$. The flux of freshwater DIC is defined as (Co × Q), whereas the flux of DIC added internally is $Q(C_s - Co)$; see Methods section for complete description. The reported annual fluxes were obtained by assuming a steady state between transects and by assuming that the July 1996 transect data was in steady state for 1 month.

Date	Equation	Co (μM)	Cs (μM)	Q ($m^3\ s^{-1}$)	Export internally added DIC (10^9 mmol d^{-1})	Export freshwater DIC (10^9 mmol d^{-1})
Jul 96	$-3.9\times S^2+121.6\times S+498.7$	499	1910	36	4.5	1.5
Sep 96	$-2.1\times S^2+97.9\times S+503.3$	503	1131	45	2.4	1.9
Nov 96	$-8.9\times S^2+75.3\times S+497.0$	497	742	75	1.9	2.9
Jan 97	$-0.8\times S^2+72.5\times S+512.2$	512	689	123	2.5	4.8
Mar 97	$73.4\times S+341.3$	341	341	114	0	3.4
Apr 97	$72.0\times S+258.0$	258	258	107	0	2.4
Jun 97	$-0.8\times S^2+66.9\times S+457.6$	458	760	45.8	1.2	1.8
Jul 97	$-1.8\times S^2+95.4\times S+391.8$	398	1210	25	1.8	7.9
Sep 97	$-2.5\times S^2+117.0\times S+343.4$	343	1654	15	1.7	5.3
Oct 97	$-2.3\times S^2+117.0\times S+260.2$	260	1523	7.6	0.8	2.4
Dec 97	$53.6\times S+543.7$	544	544	43.9	0	2.1

Total flux (10^9 mole yr^{-1}): Jan 96–Jun 97, 1.7; Dec 96–Dec 97, 2.1. Internally added flux (10^9 mole yr^{-1}): Jun 96–Jun 97, 0.6; Dec 96–Dec 97, 0.9. Conservative flux: (10^9 mole yr^{-1}): Jun 96–Jun 97, 1.1; Dec 96–Dec 97, 1.2.

DIC fluxes from the York to the lower Chesapeake Bay and estimated how much of this DIC was added within the estuary (Table 2). The total flux from the estuary for the period of June 1996 to June 1997 was 1.7×10^9 mole C yr^{-1} and was slightly higher (2.2×10^9 mole C yr^{-1}) if the period between December 1996 and December 1997 was considered. The percentage of the total flux added during estuarine transport was 38% in the June–June and 41% in the December–December intervals, respectively.

Net heterotrophy—We argue that CO_2 evasion and the export of internally produced DIC must be balanced by net heterotrophy, which can be estimated by summing these two inorganic carbon sinks. The internally produced DIC available for export (Table 2) was converted to areal estimates by dividing by the total surface area of the York River estuary. Seasonal rates of CO_2 evasion, DIC accumulation, and net heterotrophy are shown in Fig. 4. CO_2 evasion and DIC accumulation were both positive on all sampling dates, making the estuary a net heterotrophic system year-round. It is also evident from Fig. 4 that rates of CO_2 evasion and DIC accumulation were of equal importance as sinks for estuarine pCO_2, and therefore, both must be considered when calculating rates of net heterotrophy.

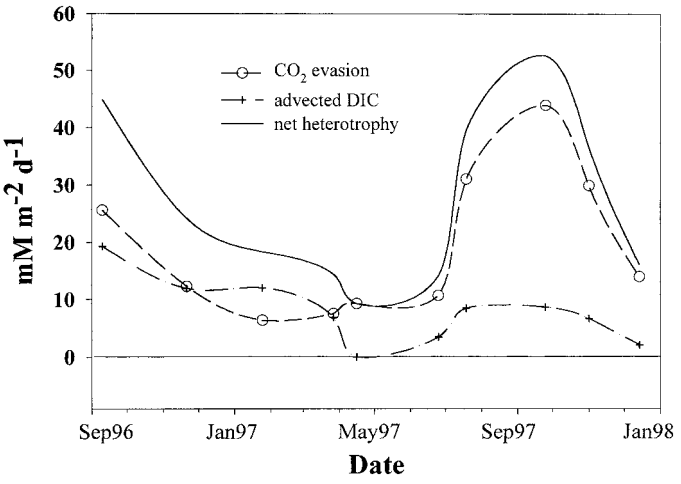

Fig. 4. Rates of whole system CO_2 evasion, DIC accumulation, and net heterotrophy in the York River estuary. All three parameters had a late summer and early fall maximum and a spring minimum. Rates of net heterotrophy were calculated by summing CO_2 evasion and DIC accumulation.

The degree of heterotrophy followed distinct patterns, with rates being highest in the late summer and fall and lowest in the late winter and early spring (Fig. 4). For the period of July 1996 to July 1997 the annual estimate of net heterotrophy was 100 g C m^{-2} yr^{-1} (29.4 mmol m^{-2} d^{-1}), but it increased to 114 g C m^{-2} yr^{-1} when the period of December 1996 to December 1997 was considered. If CO_2 supersaturation and evasion were products of net heterotrophy, we can also interpret spatial and temporal patterns in CO_2 evasion (Table 1) as indicative of spatial and temporal trends in net heterotrophy. The highest rates of net heterotrophy were in the low salinity regions (sections 4 and 5) from June through October. The lowest rates of net heterotrophy were in sections 1–3 of the estuary from November through June, and in fact, section 1 was net autotrophic from November 1996 to April 1997. The spatial and temporal dynamics of net heterotrophy are illustrative of the complex biological dynamics occurring within the estuary.

Discussion

Estimates of piston velocity—Rates of pCO_2 evasion and estimates of net heterotrophy based on pCO_2 evasion are highly dependent on the choice of k (Eq. 1). Because direct measurements of k were not available for the York, we originally relied on wind–speed relationships from literature re-

views (*see* Wanninkof 1992; Cole and Caraco 1998) to estimate k from average daily wind speeds. The average daily k_{600} values calculated with daily wind speeds and the equations offered by Wanninkhof (1992) and Cole and Caraco (1998) were 3.8 and 3.9 cm h^{-1} (i.e., 1.06 and 1.08 $\times$ 10^{-5} m s^{-1}), respectively. However, several recent estuarine studies have used k_{600} values of $\geq$8 cm h^{-1} to estimate CO_2 exchange for a number of U.S. and European rivers and estuaries (Cai and Wang 1998; Frankignoulle et al. 1998; Cai et al. 1999). For the 521 d of this study, a k_{600} value of 8 cm h^{-1} provides an average daily whole estuary flux of 27.4 mmol m^{-2} d^{-1} compared with fluxes of 11.2 and 12.2 mmol m^{-2} d^{-1} with the relationships from Wanninkhof (1992) and Cole and Caraco (1998), respectively. Frankignoulle et al. (1998) chose a value of 8 cm h^{-1} based on a number of floating dome measurements made on the same European estuaries. In their earlier work on two Georgia blackwater estuaries, Cai and Wang (1998) used an average k of 12.5 cm h^{-1}. This was the k value for Rn established for the Pee Dee River (Elsinger and Moore 1983), as derived by a ^{222}Rn mass balance approach. In contrast, for the same Georgia estuaries, Cai et al. (1999) more recently used the average k value of 8 cm h^{-1} proposed by Frankignoulle et al. (1998).

The k_{600} values used in these other studies are a factor of 2 higher than the average values established by the Wanninkhof (1992) and Cole and Caraco (1998) equations. However, these higher k_{600} values are still within the reported range of most studies that have reported values for large rivers or estuaries (Elsinger and Moore 1983; Hartman and Hammond 1984; Devol et al. 1987; Clark et al. 1992; Marino and Howarth 1993; Clark et al. 1994; Carini et al. 1996). Furthermore, the increased average k_{600} value of 8 cm h^{-1} measured by Frankignoulle et al. (1998) was believed to be associated with increased turbulence created by interactions of tidal currents with wind and bottom substrate (Frankignoulle pers. comm.). Previous workers have found that bottom-associated turbulence can control turbulence at the surface in shallow, fast-running streams and rivers (O'Connor and Dobbins 1956). In estuaries, however, turbulence associated with bottom stress will vary with depth and tidal velocity. A study by Cerco (1989) concluded that bottom-associated turbulence will be important only in shallower estuaries with high current speeds. We concur that estuarine systems may inherently have more turbulence than do other systems (i.e., lakes and oceans), thereby leading to higher k values. Nevertheless, we believe that an estimate of 8 cm h^{-1} is somewhat increased compared with those expected for average conditions on the York River estuary. We therefore chose to apply an equation based on wind speed that produced a more conservative estimate of k.

A direct and accurate method for measuring piston velocities over large temporal and spatial scales is by the addition of SF_6 (sulfur hexafluoride), because it is nonreactive and can be detected in extremely small quantities. The only two SF_6 studies on tidal systems (Clark et al. 1995; Carini et al. 1996) were conducted on temperate estuaries of varying depth and tidal velocity. Both Clark et al. (1995) and Carini et al. (1996) report k as a function of wind, and by grouping the two studies together, we obtained Eq. 2 (see Materials and methods). By using Eq. 2 and measured daily wind speeds, we obtained an average k value of 4.7 cm h^{-1} and an average daily whole-estuary flux of 16.5 mmol m^{-2} d^{-1} for the 521 d of this study.

It is possible that the actual value of k is somewhat higher than the value we chose because of chemical enhancement of CO_2 exchange (Wanninkhof and Knox 1996). Using pH, temperature, and estimated unenhanced k values (data not shown), and then calculating an enhanced k according to Wanninkhof and Knox (1996), we estimate that chemical enhancement in the York would result in k values that are no more than 11 $\pm$ 19% (average with SD, n = 72) higher than unenhanced values. Chemical enhancement of diffusion in the York is thus assumed to be negligible and not a source of bias.

pCO_2 supersaturation in estuaries—A net heterotrophic system will have R > GPP, resulting in waters that are supersaturated with respect to CO_2 (Teal and Kanwisher 1966; Smith and Hollibaugh 1993). For a given system, the magnitude of CO_2 supersaturation is affected by the degree of heterotrophy, leading to higher CO_2 concentrations during periods of greater net heterotrophy. The York River estuary is dominated by supersaturated CO_2 conditions (Fig. 2). We therefore view the predominance of supersaturation as qualitative evidence of net heterotrophy, and we use CO_2 concentrations and distributions to elucidate patterns in net heterotrophy (see below). However, first we examine other factors controlling CO_2 in estuaries.

Possible abiotic sources of inorganic carbon to the York River estuary include groundwater and $CaCO_3$ dissolution. However, the magnitude of deep groundwater flow directly to the York estuary is low, with most of it being exported to the coastal ocean (Dai pers. comm.). Similarly, the pH, Ca^{2+}, and DIC levels in the York do not indicate dissolution or even precipitation of $CaCO_3$. Even if we could argue an abiotic source of inorganic carbon to the York, it is difficult to propose an abiotic source that would create the predictable seasonal and temporal patterns witnessed in CO_2 and DIC, or to balance the large quantities of carbonate alkalinity added within the York.

High estuarine CO_2 concentrations in the York may also originate from riverine waters upstream that have not had time to de-gas. In the York, on the basis of a k of 4.7 cm h^{-1} and an average depth of 7 m, 50% equilibration with the atmosphere occurs approximately every 6 d. The flushing time of the York is 1–2 months (Sin et al. 1999), and therefore, most CO_2 lost to the atmosphere must be balanced by an internal source.

The spatial trends in pCO_2 observed in the York River estuary are qualitatively similar to those recently reported in Frankignoulle et al. (1998) and Cai and Wang (1998). Frankignoulle et al. (1998) proposed mixing of supersaturated freshwater with seawater, CO_2 efflux to the atmosphere, and marked heterotrophy in the upper estuary as major controls on the spatial distributions of pCO_2 within an estuary. In the York, the most pronounced spatial variation occurs in the summer and fall (Fig. 2), when flow rates are low and water residence times are long. As discussed earlier, the average time required for the pCO_2 in the York to reach 50% equil-

ibration with the atmosphere (average depth/$k \sim 6$ d) is a factor of 5–10 faster than freshwater residence times (1–2 months, Sin et al. 1999). This indicates that the mixing of supersaturated freshwater with seawater is too slow to create the pCO_2 distributions observed in the York River estuary, and the processes of atmospheric evasion and net heterotrophy are of greater importance.

Atmospheric efflux of CO_2 increases in the lower York because of morphological changes (i.e., increases in surface area) in the estuary. At the two end-member stations, the surface area for sections of 10 nautical miles increases from 11.3×10^6 m^2 for section 5 of our study to 58.4×10^6 m^2 for section 1. Similar morphological changes associated with funnel-shaped estuaries are found in the Scheldt (Frankignoulle et al. 1996) and the Satilla (Cai and Wang 1998), which also exhibit similar spatial patterns in pCO_2. Thus, large increases in surface area with proximity to the mouth of these estuaries would increase the importance of atmospheric exchange in the lower estuary, and they may be partially responsible for lower pCO_2 concentrations at higher salinities. The morphology of funnel-shaped estuaries would also increase the fetch at the mouth of the estuary and allow for increases in wind speed and wind-induced turbulence.

Ancillary data collected in the York are consistent with the hypothesis that marked heterotrophy in the upper estuary is partially responsible for spatial variations in pCO_2. In the upper York where CO_2 is supersaturated, phytoplankton are light-limited (Sin et al. 1999), and bacterial production is greatest (Schultz 1999). The combination of these two factors in conjunction with high rates of marsh respiration in the upper York (Neubauer et al. 2000) favor net heterotrophy, the accumulation of pCO_2, and high rates of CO_2 evasion. Interestingly, other patterns in system metabolism are consistent with pCO_2 trends in the York River estuary. Spring blooms in the York occur in the higher salinity reaches of the York (Sin et al. 1999). We speculate that these blooms create a midestuary minimum in spring pCO_2 levels (Fig. 2). The relationship between net heterotrophy and CO_2 concentrations is also evident in seasonal CO_2 oscillations. Maximum CO_2 concentrations in all five sections of the estuary occur in the summer and early fall, when water temperatures are high, favoring high rates of benthic, pelagic, and marsh respiration. Minimum CO_2 concentrations occur in the winter and spring, when water temperatures are low, spring phytoplankton blooms are common (Sin et al. 1999), and discharge is high. Similar seasonal patterns in CO_2 were observed at a heterotrophic freshwater station in the Hudson River (Raymond et al. 1997).

It is worth noting that the present study did not correct for diel fluctuations in CO_2 when calculating atmospheric flux. Instead, all CO_2 measurements were made during daylight hours. Correcting for diel variation could result in a slightly higher estimate of CO_2 evasion, particularly in the summer, because nighttime CO_2 levels are generally higher because of the absence of primary production (Raymond et al. 1997). However, limited diel studies on the York (Raymond unpublished data) concluded the range in CO_2 over a summer diel cycle ($\sim$400 ppmv) was considerably less than the observed range in seasonal ($>$2,000 ppmv) and spatial measurements ($>$2,000 ppmv).

Table 3. Average pCO_2 ranges for various United States and European estuaries. The average range was obtained by averaging the low and high concentrations for each transect, and the estuaries are ranked by the high average range.

Estuary	Number of transects	Average pCO_2 range (ppmv)
Altamaha (Georgia)*	1	380–7800
Scheldt (Belgium/Netherlands)†	10	496–6653
Sado (Portugal)†	1	575–5700
Satilla (Georgia)*	2	420–5475
Thames (U.K.)†	2	485–4900
Ems (Germany/Netherlands)†	1	560–3755
Gironde (France)†	5	499–3536
Douro (Portugal)†	1	1330–2200
York (Virginia)‡	12	352–1896
Tamar (U.K)†	2	390–1825
Hudson (N.Y.)§	6	517–1795
Rhine (Netherlands)†	3	563–1763
Rappanhannock (Virginia)‖	9	474–1613
James (Virginia)‖	10	284–1361
Elbe (Germany)†	1	580–1100
Columbia (Oregon)¶	1	560–950
Potomac (Maryland)‖	12	646–878
	Average =	531–3129

* From Cai and Wang (1998) and Cai et al. (1999).
† From Frankignoulle et al. (1998).
‡ Present study.
§ From Raymond et al. (1997).
‖ From U.S. Environmental Protection Agency data as outlined in Methods section of this paper.
¶ From Park et al. (1969).

Table 3 compares pCO_2 concentrations from various United States and European estuaries. We compare pCO_2 concentrations instead of gas fluxes because of the aforementioned uncertainties associated with comparing CO_2 flux data from studies using different k values. The York River estuary and other subestuaries from the Chesapeake Bay (i.e., the Potomac, Rappahannock, and James) fall in the low range of pCO_2 reported for estuaries. Part of the discrepancy may be because of a lack of seasonal coverage in many of the estuaries; yet, the large range in estuarine pCO_2 is probably not a function of this alone. It is probable that an important source of variation in estuarine CO_2 supersaturation is caused by large differences in organic matter concentrations between estuaries. Frankignoulle et al. (1998) stated that the European estuaries encompassed in their study were subject to increased loading of detrital organic matter from pollution. Cai and Wang (1998) reported dissolved organic carbon (DOC) concentrations in the Satilla and Altamaha rivers of 25–50 and 10 mg L^{-1}, respectively, whereas concentrations of DOC in the low salinity region of the York averaged 5 mg L^{-1} (Raymond and Bauer 2000).

If excess respiration is contributing to the excess pCO_2 in rivers and estuaries, the ultimate source of this excess CO_2 is organic carbon, which is oxidized to CO_2 by heterotrophic populations. We may therefore predict that greater DOC concentrations are correlated with higher pCO_2 concentrations. We observed a positive relationship ($r^2 = 0.75$, $P < 0.001$) between DOC and pCO_2 for six of the estuaries in Table 3,

where DOC and pCO_2 values were available. Relationships between DOC and pCO_2 have also been reported for lake systems (Hope et al. 1996; Cole 1999).

The average pCO_2 range for the 17 estuaries listed in Table 3 is 531–3,129 ppmv. Using these concentrations and an average estuarine salinity (8 ppt) and temperature (18°C) and a k_{600} of 4.7 cm h^{-1} provides a range in the rate of evasion of 2.3 moles m^{-2} yr^{-1} to 42.0 moles m^{-2} yr^{-1}. This range is a factor of 4 lower than the 36–182 moles m^{-2} yr^{-1} estimated by Frankignoulle et al. (1998) for western European estuaries alone. Approximately half of the discrepancy is a result of our study using a more conservative estimate for *k.*

On the basis of the large seasonal variation in pCO_2 concentrations in the York River estuary, it is also evident that more detailed temporal coverage is needed for accurate annual flux estimates. In particular, care must be taken to include winter measurements when reporting annual evasion rates, because estuaries exhibit a winter minimum in CO_2 concentrations (Fig. 2). In the York, if we calculated CO_2 fluxes from July 1997 to December 1997 (an incomplete annual sampling period), we would calculate an annual flux of 11.7 moles m^{-2} yr^{-1}, as opposed to 7.1 moles m^{-2} yr^{-1} for the period of December 1996 to December 1997. This equates to a factor of 1.7 difference. On the basis of the seasonal variation in pCO_2 found in the study, we stress the importance of complete temporal coverage when reporting annual integrated CO_2 fluxes in temperate estuaries.

Internally added DIC—An average (with SD) of 94 ± 6% of the DIC pool in the York River estuary comprises bicarbonate and carbonate, as determined by DIC and CO_2 measurements. Therefore, the internally added DIC that is subsequently exported via advection represents a flux of carbonate alkalinity, not dissolved CO_2 that has not had sufficient time to de-gas. This is an important distinction because the DIC/alkalinity flux represents a long-term, nonatmospheric sink for CO_2 generated during the respiration of organic matter in estuaries. In fact, because of the charge of carbonate (2−), the flux of internally produced carbonate alkalinity is slightly (~1.3%) greater than the flux of internally produced DIC (data not shown).

If, as we have argued, net heterotrophy is also the source of the DIC available for advective export from the York, DIC should exhibit similar temporal trends and be correlated to pCO_2 in the estuary. The large number of transects and stations and the predictability of DIC (see equations in Table 2) and pCO_2 in this study allowed us to establish relationships among these parameters. A significant relationship ($r^2 = 0.44$, $P < 0.05$) was found between the DIC concentration extrapolated for salinity 10 and CO_2 from salinity 5 (Fig. 5a). The pCO_2 and DIC distributions also displayed similar seasonal patterns (Fig. 5a). The strong relationship between pCO_2 and DIC concentrations in Fig. 5a is further qualitative evidence that net heterotrophy is responsible for temporal variations in both pCO_2 and DIC. Interestingly, the relationship between pCO_2 and DIC is even stronger ($r^2 = 0.80$, $P < 0.001$) when DIC at salinity 10 is plotted against pCO_2 at salinity 5 for the previous month (Fig. 5b). This is expected because there is a ~1-month time lag between water parcels at salinities 5 and 10. Similar seasonal DIC fluctuations

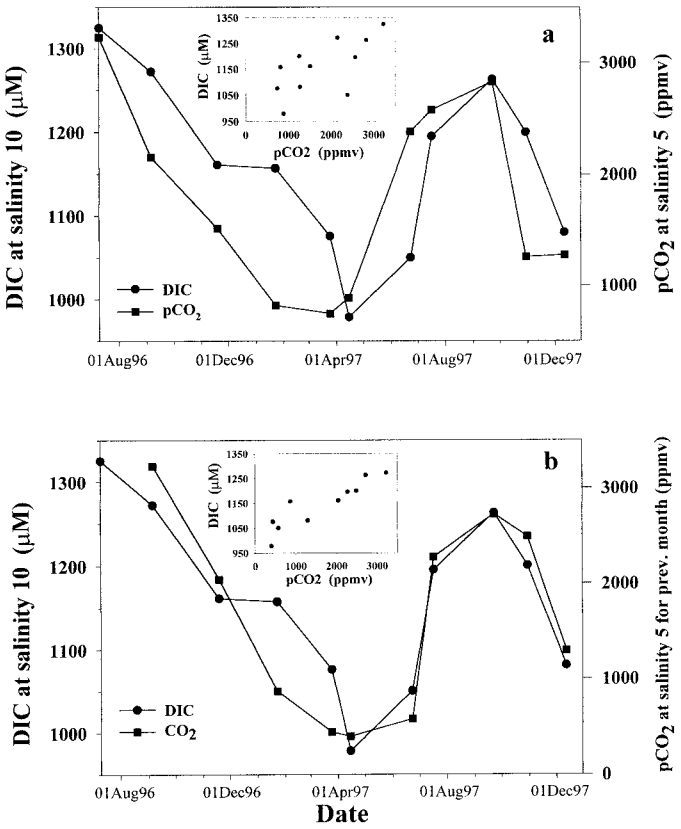

Fig. 5. (a) DIC at salinity 10 plotted against pCO_2 at salinity 5. DIC concentrations were estimated with equations in Table 2, whereas pCO_2 concentrations were estimated by assuming a linear change in pCO_2 between the two stations that bracketed salinity 5 on a given transect. (b) The same data, but DIC at salinity 10 is plotted against pCO_2 from salinity 5 from the previous month. We believe the relationship between DIC and pCO_2 is more applicable in Fig. 5b (as seen in the inserts) because it corrects for the time lag between water at salinity 10 versus salinity 5.

caused by changes in metabolic rates were found in stream and soil environments (Jones and Mulholland 1998).

We also found a significant negative relationship ($r^2 = 0.63$, $P < 0.05$) between freshwater flushing rates and DIC accumulation (data not shown). Therefore, part of the explanation for the seasonality of DIC concentration within the estuary and the seasonality of the internally produced DIC flux is from seasonal changes in freshwater residence times and flow rates. When the residence time of freshwater in the York is long, the DIC from net heterotrophy has more time to accumulate.

The conversion of CO_2 derived from net heterotrophy to carbonate alkalinity will occur only if a source of alkalinity is present. Our results indicate that the generation of alkalinity must occur at a rate of ~8 mmol m^{-2} d^{-1} to account for the internal production of DIC. Numerous microbially mediated processes, including denitrification, manganese reduction, iron reduction, and sulfate reduction, produce alkalinity by consuming H^+. Kemp et al. (1990) reported rates of denitrification of approximately 1 mmol m^{-2} d^{-1} in Chesapeake Bay sediments, which is too low to balance the nec-

essary source of alkalinity (although rates of denitrification may be higher in freshwater reaches of York).

Smith and Hollibaugh (1997) and Cai and Wang (1998) hypothesized that the source of alkalinity to the brackish and marine systems they investigated was sulfate reduction. Sulfate reduction oxidizes organic material to CO_2, using sulfate as an electron acceptor. The alkalinity produced by this process will then titrate CO_2 from respiration (aerobic or anaerobic) to HCO_3^-. As discussed in Smith and Hollibaugh (1997), net sulfate reduction is related to DIC by the following equation:

$$\text{Net sulfate reduction} = (\text{added [DIC]})/2. \quad (5)$$

Equation 5 lists net sulfate reduction, because at least part of the sulfide produced by sulfate reduction is subsequently reoxidized in a reaction that ultimately consumes a fraction of the liberated alkalinity. Total sulfate reduction, thus, will exceed net sulfate reduction (Smith and Hollibaugh 1997), and the burial or export of reduced sulfide will balance the difference between the two (total − net). For our purposes, we account for all inorganic carbon produced by the oxidation of the organic matter during sulfate reduction. The inorganic carbon from net sulfate reduction will be accounted for by the accumulation of DIC as bicarbonate because the 2 moles of alkalinity will titrate the 2 moles of CO_2 for a net gain of 2 moles of DIC. The balance (total sulfate reduction − net sulfate reduction) will be accounted for by the accumulation of DIC as CO_2 because the alkalinity formed by sulfate reduction will be lost during the reoxidation of the reduced sulfide.

Roden and Tuttle (1993) measured rates of total sulfate reduction in Chesapeake Bay sediments adjacent to the York River estuary. They report average total summer sulfate reduction rates of around 40 mmol S m^{-2} d^{-1}. If we assume sulfate burial rates of 30% of total sulfide production (Roden and Tuttle 1993), this will produce net sulfate reduction rates of around 12 mmol S m^{-2} d^{-1}, or 24 mmol C m^{-2} d^{-1} (Eq. 5). These rates are high enough to balance the advective export of internally produced DIC reported in Fig. 4. Spatial variation in sulfate reduction rates in estuaries is highly variable with maximum rates in salt marsh sediments and shallow subtidal areas (Howarth 1984), but it is evident that rates of net sulfate reduction in these areas could balance the alkalinity source necessary for DIC accumulation. It is worth noting that Abril et al. (1999) recently measured alkalinity generation at the maximum turbidity zone in the Gironde estuary. These workers proposed that in the Gironde, 14% of the total HCO_3^- exported to the coastal ocean was produced in the maximum turbidity zone, and a significant percentage of the generated HCO_3^- was balanced by denitrification and manganese reduction.

Net heterotrophy in the York River estuary—The net heterotrophic nature of coastal and estuarine systems has been proposed by a number of workers (Smith and Mackenzie 1987; Smith and Hollibaugh 1993; Heip et al. 1995; Gattuso et al. 1998). The most recent summary of net heterotrophy in estuaries and shallow coastal systems provides an average rate of net heterotrophy of 72 ± 100 g of C m^{-2} yr^{-1} for 21 systems (Gattuso et al. 1998). Our estimate of 100 g C m^{-2} yr^{-1} for the York is slightly higher than the average estuary, yet well within the reported range of Gattuso et al. (1998). The organic matter fueling net heterotrophy in the York was not produced autochthonously during the 1.5-yr study. Fluxes of total organic carbon into the freshwater portion of the York during the same time period averaged ~20 g C m^{-2} yr^{-1}, indicating that allochthonous freshwater organic carbon transported to the York during this study cannot account for a large percentage of net heterotrophy. It is possible that on longer time scales, the York is more closely balanced, and that during our study, net heterotrophy was supported by phytoplankton organic matter deposited in previous years. The York may also receive inputs of labile allochthonous organic matter from its associated marshes or the lower Chesapeake Bay, which is net autotrophic (Kemp et al. 1997). Yet another possibility is that the York imports dissolved inorganic carbon from respiration in flooded marsh waters and marsh sediments during tidal inundation of marshes by estuarine waters (Cai et al. 1999).

A current paradigm is that CO_2 evasion balances net heterotrophy in estuaries. In accordance with Smith and Hollibaugh (1997), we show in this study that another sink, the conversion of CO_2 to bicarbonate, may be quantitatively important in systems in which significant sulfate reduction occurs. Our method for calculating net heterotrophy is relatively simple and straightforward if ancillary data, such as river discharge, depth, and surface area or volume exist.

References

ABRIL, G., AND OTHERS. 1999. Oxic/anoxic oscillations and organic carbon mineralization in an estuarine maximum turbidity zone (The Gironde, France). Limnol. Oceanogr. **44:** 1304–1315.

CAI, W.-J., AND Y. WANG. 1998. The chemistry, fluxes, and sources of carbon dioxide in the estuarine waters of the Satilla and Altamaha Rivers, Georgia. Limnol. Oceanogr. **43:** 657–668.

———, POMEROY, L. R., M. A. MORAN, AND Y. WANG. 1999. Oxygen and carbon dioxide mass balance for the estuarine-intertidal marsh complexes of five rivers in the southeastern U.S. Limnol. Oceanogr. **44:** 639–679.

CARINI, S., AND OTHERS. 1996. Gas exchange in the Parker Estuary, MA. Bio. Bull. **191:** 333–334.

CERCO, C. F. 1989. Estimating estuarine reaeration rates. J. Env. Eng. **115:** 1066–1070.

CLARK, J. F., J. SIMPSON, W. M. SMETHIE, AND C. TOLES. 1992. Gas exchange in a contaminated estuary inferred from chlorofluorocarbons. Geophys. Res. Lett. **19:** 1133–1136.

———, WANNINKHOF, R., P. SCHLOSSER, AND H. J. SIMPSON. 1994. Gas exchange rates in the tidal Hudson River using a dual tracer technique. Tellus **46b:** 274–285.

CLOERN, J. E. 1987. Turbidity as a control on phytoplankton biomass and productivity in estuaries. Cont. Shelf Res. **7:** 1367–1381.

COLE J. J. 1999. Aquatic microbiology for ecosystem scientists: New and recycled paradigms in ecological microbiology. Ecosystems **2:** 215–225.

———, AND N. F. CARACO. 1998. Atmospheric exchange of carbon dioxide in a low-wing oligotrophic lake measured by the addition of SF_6. Limnol. Oceanogr. **43:** 647–656.

———, N. F. CARACO, G. W. KLING, AND T. K. KRATZ. 1994. Carbon dioxide supersaturation in the surface waters of lakes. Science **265:** 1568–1570.

CRONIN, W. B. 1971. Volumetric, areal, and tidal statistics of the

Chesapeake Bay Estuary and its tributaries. Chesapeake Bay Institute/The Johns Hopkins University, Baltimore, Maryland.

DEVOL, A. H., P. E. QUAY, J. E. RICHEY, AND L. A. MARTINELLI. 1987. The role of gas exchange in the inorganic carbon, oxygen, and 222Rn budgets of the Amazon River. Limnol. Oceanogr. **32:** 235–248.

DOUMELELE, D. G. 1979. New Kent County tidal marsh inventory. 208, Virginia Institute of Marine Science/College of William and Mary, Gloucester Point.

DUCKLOW, H. W. 1982. Chesapeake Bay nutrient and plankton dynamics. 1. Bacterial biomass and production during spring tidal destratification in the York River, Virginia. Limnol. Oceanogr. **27:** 651–659.

ELSINGER, R. J., AND W. S. MOORE. 1983. Gas exchange in the Pee Dee River based on ^{222}RN evasion. Geophys. Res. Lett. **10:** 443–446.

FRANKIGNOULLE, M., I. BOURGE, AND R. WOLLAST. 1996. Atmospheric CO_2 fluxes in a highly polluted estuary (the Scheldt). Limnol. Oceanogr. **41:** 365–369.

———, AND OTHERS. 1998. Carbon dioxide emission from European estuaries. Science **282:** 434–436.

GATTUSO, J.-P., M. FRANKIGNOULLE, AND R. WOLLAST. 1998. Carbon and carbonate metabolism in coastal aquatic ecosystems. Annual review of ecology and systematics. Annu. Rev., Palo Alta, California, 405–434 pp.

HAAS, L. W., S. J. HASTINGS, AND K. L. WEBB. 1981. Phytoplankton response to a stratification-mixing cycle in the York River estuary during late summer, p. 619–636. *In* B. J. Neilson and L. E. Cronin [eds.], Estuaries and nutrients. Humana.

HARTMAN, B., AND D. E. HAMMOND. 1984. Gas exchange across the sediment-water and air-water interfaces in south San Francisco Bay. J. Geophys. Res. **89:** 3593–3603.

HEIP, C. H., AND OTHERS. 1995. Production and consumption of biological particles in temperate tidal estuaries. Oceanography and marine biology: An annual review. UCL.

HOPE, D., T. K. KRATZ, AND J. L. RIERA. 1996. Relationship between pCO_2 and dissolved organic carbon in Northern Wisconsin Lakes. J. Env. Qual. **25:** 1442–1445.

HOPKINSON, C. S., AND J. J. VALLINO. 1995. The relationships among man's activities in watersheds and estuaries: A model of runoff effects on patterns of estuarine community metabolism. Estuaries **18:** 598–621.

HOWARTH, R. W. 1984. The ecological significance of sulfur in the energy dynamics of salt marsh marine ecosystems. Biogeochemistry **1:** 5–27.

JAHNE, B., G. HEINZ, AND W. DIETRICH. 1987. Measurements of the diffusion coefficients of sparingly soluble gases in water. J. Geophys. Res. **92:** 10767–10776.

JONES, J., AND P. MULHOLLAND. 1998. Carbon dioxide variation in a hardwood forest stream: An integrative measure of whole catchment soil respiration. Ecosystems **1:** 189–196.

KAUL, L. W., AND P. N. FROELICH, JR. 1984. Modelling estuarine nutrient geochemistry in a simple system. Geochim. Cosmochim. Acta **48:** 1417–1433.

KEMP, W. M., P. SAMPOU, J. CAFFREY, AND M. MAYER. 1990. Ammonia recycling versus denitrification in Chesapeake Bay sediments. Limnol. Oceanogr. **35:** 1545–1563.

———, E. SMITH, M. MARVIN-DIPASQUALE, AND W. R. BOYNTON. 1997. Organic carbon balance and net ecosystem metabolism in Chesapeake Bay. Mar. Ecol. Prog. Ser. **150:** 229–248.

KOEPFLER, E. T. 1989. Heterotrophic bacterial production: Relationships to biological and abiological factors in estuarine environments. Ph.D. thesis, College of William and Mary, Gloucester Point, Virginia.

LODER, T. C., AND R. P. REICHARD. 1981. The dynamics of conservative mixing in estuaries. Estuaries **1:** 64–69.

MAGNIEN, R. E., R. M. SUMMERS, AND K. G. SELLNER. 1992. External sources, internal nutrient pools, and phytoplankton production in Chesapeake Bay. Estuaries **15:** 497–516.

MARINO, R., AND R. W. HOWARTH. 1993. Atmospheric oxygen exchange in the Hudson River: Dome measurements and comparison with other natural waters. Estuaries **16:** 433–445.

MAYER, L. M., AND OTHERS. 1998. Importance of suspended particulates in riverine delivery of bioavailable nitrogen to coastal zones. Global Biogeoch. Cycles **12:** 573–579.

MILLERO, F. J. 1995. Thermodynamics of the carbon dioxide system in the oceans. Geochim. Cosmochim. Acta **59:** 661–677.

NEUBAUER, S. C., W. D. MILLER, AND I. C. ANDERSON. 2000. Carbon cycling in a tidal freshwater marsh ecosystem: A carbon gas flux study. Mar. Ecol. Prog. Ser. **199:** 13–30.

O'CONNOR, D., AND W. DOBBINS. 1956. Mechanism of reaeration in natural streams. J. San. Eng. **82:** 1115–1128.

OFFICER, C. B. 1979. Discussion of the behavior of nonconservative dissolved constituents in estuaries. East Coast Mar. Sci. **9:** 91–94.

PARK, P. K., S. W. HAGER, AND M. C. CISSELL. 1969. Carbon dioxide partial pressure in the Columbia River. Science **166:** 867–868.

RAYMOND, P. A., N. F. CARACO, AND J. J. COLE. 1997. Carbon dioxide concentration and atmospheric flux in the Hudson River. Estuaries **20:** 381–390.

———, AND J. E. BAUER. 2000. Bacterial consumption of DOC during transport through a temperate estuary. Aquat. Microb. Ecol. **22:** 1–12.

RODEN, E. E., AND J. H. TUTTLE. 1993. Inorganic sulfur cycling in mid and lower Chesapeake Bay sediments. Mar. Ecol. Prog. Ser. **93:** 101–118.

SCHULTZ, G. E. 1999. Bacterial dynamics and community structure in the York River estuary. Ph.D. dissertation, Virginia Institute of Marine Science/College of William and Mary, Gloucester Point.

SHOLKOVITZ, E. R., E. A. BOYLE, AND N. B. PRICE. 1978. The removal of dissolved humic acids and iron during estuarine mixing. Earth Planet. Sci. Lett. **40:** 130–136.

SILBERHORN, G. M., AND A. W. ZACHERLE. 1987. King William County and town of West Point tidal marsh inventory. Virginia Institute of Marine Science/College of William and Mary, Gloucester Point.

SIN, Y., R. L. WETZEL, AND I. C. ANDERSON. 1999. Spatial and temporal characteristics of nutrient and phytoplankton dynamics in the York River. Estuaries. **22:** 260–275

SMITH, S. V., AND J. T. HOLLIBAUGH. 1993. Coastal metabolism and the oceanic organic carbon balance. Rev. Geophys. **31:** 75–89.

———, AND ———. 1997. Annual cycle and interannual variability of ecosystem metabolism in a temperate climate embayment. Ecol. Monogr. **67:** 509–533.

———, AND F. T. MACKENZIE. 1987. The ocean as a net heterotrophic system: Implications from the carbon biogeochemical cycle. Global Biogeochem. Cycles **1:** 187–198.

TEAL, J. M., AND J. KANWISHER. 1966. The use of pCO_2 for the calculation of biological production, with examples from waters off Massachusetts. J. Mar. Res. **24:** 4–14.

WANNINKHOF, R. 1992. Relationship between wind speed and gas exchange over the ocean. J Geophys. Res. **97:** 7373–7382.

———, AND M. KNOX. 1996. Chemical enhancement of CO_2 exchange in natural waters. Limnol. Oceanogr. **41:** 689–697.

Received: 18 October 1999
Accepted: 20 June 2000
Amended: 8 August 2000